HHS Public Access

Author manuscript

Epilepsy Res. Author manuscript; available in PMC 2020 August 01.

Published in final edited form as:

Epilepsy Res. 2019 August ; 154: 132–138. doi:10.1016/j.eplepsyres.2019.05.006.

Inhibition of T-Type Calcium Channels in mEC Layer II Stellate Neurons Reduces Neuronal Hyperexcitability Associated with Epilepsy.

Aradhya Nigam[1], **Nicholas J. Hargus**[1,2], **Bryan S. Barker**[1,2], **Matteo Ottolini**[1], **James A. Hounshell**[1,2], **Edward H. Bertram III**[3,2], **Edward Perez-Reyes**[4,2], and **Manoj K. Patel**[1,2,#]

[1]Department of Anesthesiology, University of Virginia Health System, Charlottesville, VA 22908, USA.

[2]Department of Neuroscience Graduate Program, University of Virginia Health System, Charlottesville, VA 22908, USA.

[3]Department of Neurology, University of Virginia Health System, Charlottesville, VA 22908, USA.

[4]Department of Pharmacology, University of Virginia Health System, Charlottesville, VA 22908, USA.

Abstract

Temporal lobe epilepsy (TLE) is a form of adult epilepsy involving the entorhinal cortex (EC). Layer II neurons of the medial EC (mEC) are spared and become hyperexcitable in TLE. Studies have suggested a role for T-type calcium channels (T-type Ca^{2+} channels) in facilitating increases in neuronal activity associated with TLE within the hippocampus. We sought to determine if T-type Ca^{2+} channels play a role in facilitating neuronal hyperexcitability of layer II mEC stellate neurons in TLE.

TLE was induced in rats by electrical stimulation of the hippocampus to induce *status epilepticus* (*SE*). Brain slices were prepared from rats exhibiting spontaneous seizures and compared with age-matched control rats. Action potentials (APs) were evoked either by current injection steps or via presynaptic stimulation of mEC deep layers. The selective T-type Ca^{2+} channel antagonist, TTA-P2 (1 μM), was applied to determine the role of T-type Ca^{2+} channels in maintaining neuronal excitability. Quantitative PCR techniques were used to assess T-type Ca^{2+} channel isoform mRNA levels within the mEC layer II.

TLE mEC layer II stellate neurons were hyperexcitable compared to control neurons, evoking a higher frequency of APs and generating bursts of APs when synaptically stimulated. TTA-P2 (1 μM) reduced firing frequencies in TLE and control neurons and reduced AP burst firing in TLE stellate neurons. TTA-P2 had little effect on synaptically evoked AP's in control neurons. TTA-P2

[#]**Corresponding Author:** Manoj K. Patel, Department of Anesthesiology, Box 800710, University of Virginia Health System, Charlottesville VA, 22908-0710, USA., Tel: +1 434 924 9693, Fax: +1 434 924 2105, (mkp5u@virginia.edu).

Declaration of Interest: The authors have no disclosures to report.

also inhibited rebound APs evoked in TLE neurons to a greater degree than in control neurons. TLE tissue had almost a 3-fold increase in $Ca_v3.1$ mRNA compared to controls. $Ca_v3.2$ or $Ca_v3.3$ levels were unchanged.

These findings support a role for T-type Ca^{2+} channel in establishing neuronal hyperexcitability of mEC layer II stellate neurons in TLE. Increased expression of $Ca_v3.1$ may be important for establishing neuronal hyperexcitability of mEC layer II neurons in TLE.

Keywords

T-type calcium channel; Temporal Lobe Epilepsy; Entorhinal Cortex; Stellate Neurons

1. Introduction

Temporal lobe epilepsy (TLE) is one of the most common human epileptic disorders, and the clinical manifestations of this disease can be induced through a variety of brain insults. Limbic structures of the temporal lobe, including the entorhinal cortex (EC) are known to be involved in initiating seizure activity in humans (Avoli et al., 2002; Curia et al., 2014).

Spontaneous seizures have been recorded from the EC in patients (Spencer and Spencer, 1994) and stimulation of the EC in patients evokes spontaneous interictal spikes in the hippocampus (Rutecki et al., 1989). Surgical resection of the EC is also effective in suppressing seizures (Siegel et al., 1990). In animal models of epilepsy, mEC layer II neurons are spared and become hyperexcitable, displaying prolonged excitatory synaptic responses to stimulation of the EC deep layers (Bear et al., 1996; Hargus et al., 2011). Layer II stellate neurons form the major excitatory input into the dentate gyrus (DG) and CA1 via the perforant path and the temporoammonic path respectively (Segal and Landis, 1974). Increased neuronal activity of EC layer II neurons ultimately leads to an excessive excitatory input onto DG neurons of the hippocampus, further exciting the network (Kobayashi et al., 2003).

Voltage gated T-type Ca^{2+} channels are low threshold activated ion channels and are thought to play an important role in controlling neuronal excitability (Llinás, 1988). All three T-type Ca^{2+} channel isoforms, $Ca_v3.1$, $Ca_v3.2$ and $Ca_v3.3$ are expressed within the central nervous system (CNS) (Talley et al., 1999). The role of T-type Ca^{2+} channels in absence epilepsy has been extensively studied. In T-type Ca^{2+} channel animal models of absence epilepsy (GAERS and WAG/Rij rats) increased T-type Ca^{2+} channel expression and currents have been reported and associated with the appearance of spike-wave discharges characteristic of absence seizures (Talley et al., 2000; Tsakiridou et al., 1995). Recent studies also implicate a role for T-type Ca^{2+} channels in TLE. T-type Ca^{2+} channel currents are upregulated in pyramidal neurons of the CA1 in a pilocarpine rat model of epilepsy, accounting for the switch from tonic AP firing in control neurons to low threshold bursting APs in TLE neurons (Su et al., 2002). The upregulation of T-type Ca^{2+} channel is likely at the apical dendrites since focal inhibition of these channels at these distant sites leads to a suppression of epileptiform burst firing of CA1 neurons (Yaari et al., 2007). Within the hippocampus, $Ca_v3.2$ mRNA and protein levels are increased after pilocarpine induced SE, however the

increase is only transient and returns to control levels 10 days after *SE* and before the onset of spontaneous seizures (A J Becker et al., 2008). Interestingly, $Ca_v3.2$ deficient mice had reduced neuronal loss and mossy fiber sprouting. Additionally, these mice also had reduced spontaneous seizures, suggesting that although the upregulation of $Ca_v3.2$ was transient, sustained alterations persisted. $Ca_v3.1$ has been associated with seizures in a kainic acid model of TLE. $Ca_v3.1$ deficient mice had significantly reduced seizure duration, but an increase in seizure frequency (Kim, 2015). Inhibition of T-type Ca^{2+} channels prevented tonic-clonic seizures in the maximal electroshock seizure model (Sakkaki et al., 2016) and delayed progression of seizures in an amygdala kindled model of TLE (Casillas-Espinosa et al., 2015). These studies provide support for a role of T-type Ca^{2+} channels in the development of various forms of epilepsy.

While alterations in T-type Ca^{2+} channels within the hippocampus have been extensively studied, the mEC has received limited attention. In this study, we confirm that mEC layer II stellate cells are hyperexcitable in TLE compared to controls. We show that application of the selective T-type Ca^{2+} channel blocker, TTA-P2 significantly reduces firing rates in TLE neurons to control levels and suppresses synaptically evoked burst firing. TTA-P2 also profoundly inhibited rebound firing in TLE neurons over controls. qPCR revealed a three-fold increase in $Ca_v3.1$ message, but no change in $Ca_v3.2$ or $Ca_v3.3$ message in TLE. These results suggest that upregulation of T-type Ca^{2+} channel isoforms may be regionally specific between the mEC and the hippocampus. As such, selective T-type Ca^{2+} channel blockers may be a promising option for rational anti-epileptic drug design in TLE.

2. Material and methods

2.1 TLE model preparation

All animal experiments were conducted in accordance with the guidelines established by the National Institutes of Health guide for the Care and Use of Laboratory Animals and were approved by the University of Virginia's Institute of Animal Care and Use Committee. Details regarding electrode implantation, stimulation and seizure monitoring have been published previously (Hargus et al., 2013, 2012, 2011). In brief, adult male Sprague-Dawley rats were implanted with a pair of stainless steel electrodes unilaterally to the left hemisphere. One week following surgery, rats were stimulated for 90 minutes with 10 second trains of 50 Hz, 1 ms biphasic square waves with a maximum intensity of 400 μA peak to peak delivered every 11 seconds through the electrode to induce limbic *status epilepticus* (SE). After 90 minutes, stimulation was stopped and hippocampal activity was recorded for a minimum of 8 hours to ensure that a prolonged period of continuous EEG seizure activity was maintained. Animals that exhibited continuous electrographic seizure activity for at least 8 hours after stimulation were at uniform risk for development of limbic epilepsy. Animals (about 15%) that did not meet the EEG criteria of minimum continuous seizure activity were not maintained, as their chance of developing chronic epilepsy was extremely low. At least two months after the induction of SE, animals were evaluated for the presence of spontaneous temporal lobe seizures, as the seizure pattern and frequency typically stabilizes by this time (Bertram and Cornett, 1993). Approximately 80% of animals monitored developed epilepsy.

2.2 Entorhinal cortex slice preparation

Horizontal brain slices (300 μm) were prepared from Sprague Dawley rats (250-400 grams; with TLE (n = 21) or aged matched controls (n = 12). Animals were euthanized with isoflurane, decapitated, and their brains were rapidly removed and submerged in ice cold artificial cerebral spinal fluid (ACSF) containing (in mM): 125 NaCl, 2.5 KCl, 1.25 NaH_2PO_4, 2 $CaCl_2$, 1 $MgCl_2$, 0.5 L-ascorbic acid, 2 pyruvate, 10 glucose, and 25 $NaHCO_3$ (oxygenated with 95% O_2 and 5% CO_2). Slices were prepared using a Vibratome (Vibratome 1000 Plus), transferred to a chamber containing oxygenated ACSF, incubated at 37°C for 35 min, and then stored at room temperature. In order to preserve an intact mEC, slices were obtained from 3.9 to 5.9 mm interaural (corresponding to −6.1 to −4.1 mm from bregma), and placed in numbered sub-chambers to maintain anatomical positioning of the slice. For recordings, slices were held in a small chamber superfused with heated (32°C) oxygenated ACSF at 3 mL/min. mEC layer II stellate neurons were visually identified within the EC layer II band by infra-red video microscopy (Hamamatsu, Shizouka, Japan) using a Zeiss Axioscope microscope (Zeiss, Oberkochen, Germany) and confirmed by their unique AP firing characteristics as described previously (Hargus et al., 2011). Whole-cell current clamp recordings were performed using an Axopatch 700B amplifier (Molecular Devices) using pCLAMP 10 software (Molecular Devices) and a Digidata 1322A (Molecular Devices). Electrodes were fabricated from borosilicate glass using a Brown-Flaming puller (model P97, Sutter Instruments Co). Electrodes (3.0 – 3.5 MΩ) were filled with (in mM): 120 Kgluconate, 10 NaCl, 2 $MgCl_2$, 0.5 K_2EGTA, 10 HEPES, 4 Na_2ATP, 0.3 NaGTP (pH adjusted to 7.2 with KOH). APs were evoked using current injection steps from −20 pA to 470 pA in 10 pA steps for 300 ms at 5 sec inter-pulse intervals. To standardize our tests the resting membrane potential (RMP) was recorded and then maintained at −65 mV by injection of DC current. Cell input resistance (IR) was calculated by dividing the steady-state voltage response evoked by varying current injections (ΔV/ΔI) from −20 pA until the current pulse just prior to that which evoked an AP. Data points were then fit with a linear line to determine IR values. Threshold was determined as the voltage at which the slope of the AP exceeded ≥ 20 Vs–1. AP amplitudes were measured from threshold to the AP peak. Upstroke velocity was determined from phase plots using the maximum of the first derivative (dV/dt). APs were also evoked using a stimulating electrode (WPI, Sarasota, FL, USA) placed in layer III of the mEC. A 400 μs stimulus of varying current amplitude (1 to 3.2 mA) was applied every 15 sec via a digital stimulator (Digitimer Ltd, Hertfordshire, UK). In order to consistently evoke APs the stimulus amplitude was increased 1.5 times from threshold.

To evoke rebound APs, neurons were subjected to a series of hyperpolarizing current injection steps from −100 to −1000 pA in 50 pA steps for 500 ms at 5 sec interpulse intervals followed by a 500 ms step to 0 pA current injection to evoke the rebound AP. Once the threshold was established, the time dependency of hyperpolarization-induced rebound firing was assessed by hyperpolarizing the neuron past its threshold value for varying times (150-1000 ms at 50 ms intervals) followed by a 500 ms step to 0 pA to evoke the rebound AP.

2.3 Voltage-clamp electrophysiology

Slices marked for voltage-clamp experiments were first pre-incubated in ACSF containing: 50 μM nifedipine, 1 μM conotoxin GVIA, 5 μM conotoxin MVIIC, and 0.1 μM TTX for 45 min in order to block non-T-type Ca^{2+} and sodium currents. All T-type Ca^{2+} current recordings were recorded in the intact brain slice preparation constantly superfused in oxygenated bath solution containing (in mM): 90 $CholineCl_2$, 30 TEA, 1 $MgCl_2$, 4 4-AP, 25 Glucose, 25 $NaHCO_3$, 1.25 NaH_2PO_4, 2.5 KCl, 2 $CaCl_2$, 0.001 TTX (pH 7.4 with 95% O_2, 5% CO_2). Currents were recorded using the whole-cell configuration of the patch clamp recording technique as described earlier. Electrodes had resistances of 2.2 – 3.0 MΩ when filled with an intracellular recording solution containing (in mM): 130 TMA-OH, 10 EGTA, 40 HEPES, 2 $MgCl_2$ and .005 QX-314 (pH 7.25 with 1M HF). All experiments were performed at 32°C. Capacitive and leak currents were subtracted using P/N-4 protocol. Recording ionic currents from brain slices is problematic and open to space clamp problems, due to extensive neuron processes that compromise voltage control. To minimize these problems, we only recorded from neurons where there were no extensive delays in the exponential rise of the current (within 5 ms).

The current voltage relationship was determined using a 400 ms voltage pulse from −80 to +110 mV in steps of 10 mV from a holding potential of −90 mV at 2s intervals. Conductance as a function of voltage was derived from the current-voltage relationship using the equation $g = l_{Ca}/(V\text{-}E_{Ca})$, where V is the test potential and E_{Ca} is the reversal potential. The voltage dependence of activation and inactivation data was fitted by a Boltzmann function:

$$y = 1 / (1 + \exp(V - V_{1/2}) / k)$$

where y is the normalized conductance (g/g_{max}) or the normalized current for activation and inactivation respectively, $V_{1/2}$ is voltage of half-maximal activation or inactivation and k is the slope factor.

For steady-state inactivation, neurons were held at a potential of −90 mV and test potentials from −115 mV to −45 mV for 3.5 sec at 5 mV increments were applied. The second pulse to −35 mV for 300 ms was used to assess channel availability. For each neuron, currents during the second pulse were normalized so that the largest current was 1.0 and fit to the Boltzmann function.

2.4 qPCR experiments

Three control rats and three with TLE were sacrificed and their brains removed. 300 μm horizontal slices were prepared as described earlier. Slices used corresponded to −6.1 to −4.1 mm dorsal/ventral from bregma. Under a low power microscope the mEC layer II (the area between 8 - 9 mm posterior and 4 - 6 mm lateral from Bregma) was identified as a translucent band and dissected free using a fine dissecting tool and immediately homogenized in lysis buffer. RNA was isolated using the RNAqueous 4PCR Kit (Applied Biosystems), then treated with DNAse to remove genomic DNA. cDNA was prepared with the iScript cDNA Synthesis Kit (Bio-Rad) using 10 ng of RNA per 1 μL cDNA reaction.

PCR was then carried out to measure Cav 3.1, 3.2, and 3.3 isoforms. Primer sequences used for Cav 3.1 were (from 5' to 3'), forward; TGG TCG GCC TAT ATC TTT CC, and reverse; AGA TGA TGA CGA GGA CCA CA. Primer sequences used for Cav 3.2 were (from 5' to 3'), forward; CAA GTA CTT CAA CCG AGG CA, and reverse; AAC ATG CTG GTG AAC ACG AT. Primer sequences used for Cav3.3 were (from (5' to 3'), forward; CAA CCC TGA CGT CCC ACA TCC A, and reverse; ACG GTC CGA CAG GCA CTC CAT. The cytoskeleton component β-tubulin III was also measured as a control and its primer sequences were (from 5' to 3'), forward; GCA TGG ATG AGA TGG AGT TCA CC, and reverse; CGA CTC CTC GTC GTC ATC TTC ATA C. To quantify mRNA levels, a quantitative PCR assay was conducted using the double-stranded DNA dye iQ SYBR Green Supermix (Bio-Rad) using 1 μL cDNA per 25 μL reaction. Change in cycle threshold (deltaCt) between control and TLE tissue was determined by the following equation:

$$\text{deltaCt} = (\text{Ct of Cav3.X in control} - \text{Ct of } \beta\text{-tublll in control}) - (\text{Ct of Cav3.X in TLE} - \text{Ct of } \beta\text{-tublll in TLE}).$$

Average Ct values were as follows: β-tublll, 21.1; Cav3.1, 25.7; Cav3.2, 24.9; and Cav3.3, 33.8. Melting curve analysis revealed a single peak for all primers used, thus confirming the absence of primer-dimers in the PCR products. PCR products were also separated on an agarose gel, purified, and sequenced using the forward primer to confirm product.

2.5 Drugs

2,3-Dioxo-6-nitro-1,2,3,4-tetrahydrobenzo[f]quinoxaline-7-sulfonamide (NBQX), D-(−)-2-Amino-5-phosphonopentanoic acid (AP5), strychnine, picrotoxin, tetraethylammonium (TEA), 4-aminopyradine (4-AP), tetrodotoxin (TTX), nifedipine, ω-conotoxin GVIA, ω-conotoxin MVIIC, lidocaine N-ethyl bromide (QX-314), was obtained from Sigma Aldrich (St. Louis, MO, USA). TTX, nifedipine, ω-conotoxin GVIA, ω-conotoxin MVIIC, QX-314, and nickel were prepared as 1000X stock solutions. Nifedipine, and QX-314 were prepared in DMSO. TTX was prepared in water. Stock solutions of ω-conotoxin GVIA and ω-conotoxin MVIIC were prepared in deoxygenated solution containing 0.1% BSA, 100 mM NaCl, 10 mM Trizma, and 1 mM EDTA, pH 7.5. Drugs were then diluted to working concentrations directly preceding experiments. TTA-P2 was obtained from Alomone Labs.

2.6 Data analysis

Electrophysiology data analysis was performed using Clampfit software (v10, Molecular Devices) and Origin (v6, Microcal Software). All values represent means ± standard error of the mean (S.E.M). Normality was determined using a Kolmogorov-Smirnov test. Statistical significance was determined by using a Student's *t*-test (unpaired) or a standard one-way ANOVA followed by Tukey's *post hoc* test (SigmaPlot).

3. Results

3.1 TTA-P2 reduces hyperexcitability of mEC layer II stellate neurons in TLE

mEC layer II stellate neurons were visually identified within the EC layer II band using infrared video microscopy and confirmed by their unique AP firing characteristics as described previously (Hargus et al., 2011). Consistent with our previous findings, mEC layer

II stellate neurons from epileptic animals (TLE) had significantly increased AP firing rates as compared to controls. At a current injection step of 280 pA, AP rates were increased from 15.6 ± 1.5 Hz (n = 16) in control neurons to 22.2 ± 2.1 Hz (n = 13) in TLE neurons ($P <$ 0.05 Students *t*-test; Figure 1 A). Representative traces at various current injection steps are shown in figure 1D and E. Analysis of passive and AP properties revealed a significant decrease in threshold and rheobase, and an increase in upstroke velocity in TLE neurons compared with control (Table 1). To determine the importance of T-type Ca^{2+} channels in facilitating the increase in neuronal excitability in TLE, we applied the T-type Ca^{2+} channel specific blocker, TTA-P2 at a concentration reported to abolish T currents (1 μM) (Dreyfus et al., 2010). Bath application of 1 μM TTA-P2 significantly reduced AP discharge in both control and TLE neurons (Figure 1B, C). In control neurons, application of TTA-P2 reduced firing rates from 15.6 ± 1.5 Hz (n = 16) to 9.5 ± 2.7 Hz (n = 7, $P < 0.05$ Students *t*-test). In TLE neurons, TTA-P2 reduced the firing rate from 22.2 ± 2.1 Hz (n = 13) to 10.0 ± 2.2 Hz (n = 8, $P < 0.01$ Students *t*-test). In the presence of TTA-P2, TLE neuron firing frequencies were no longer significantly different from control firing frequencies. Application of TTA-P2 did significantly increase AP thresholds to more depolarized potentials in both control and TLE neurons (Table 1), consistent with the contribution of T-type Ca^{2+} channels in establishing sub-threshold depolarizing currents (Yaari et al., 2007).

3.2 TTA-P2 reduces synaptically evoked burst firing in TLE neurons.

Brief stimulation of mEC layer III consistently evoked depolarizing potentials in mEC layer II stellate neurons that elicited single APs in control tissue (n = 6; Figure 1 F). In contrast, presynaptic stimulation evoked larger amplitude responses that elicited bursts of 2.8 ± 0.3 APs (n = 9) in TLE neurons ($P < 0.05$, one-way ANOVA; Figure 1G). The duration of the evoked depolarizing event was increased from 21.7 ± 8.1 ms (n = 9) in control to 100.7 ± 6.0 ms (n = 9) in TLE, but did not reach significance ($P < 0.05$, one-way ANOVA). Application of 1 μM TTA-P2 had no effect on synaptically evoked AP frequency or duration in control neurons (n = 6, Figure 1F). In contrast, TTA-P2 (1 μM) application reduced the bursts of synaptically evoked APs in TLE neurons to single APs (1.0 ± 0.0; n = 7, $P < 0.05$ one-way ANOVA). TTA-P2 application also reduced the duration of the evoked depolarizing potential in TLE neurons to 54.0 ± 17.5 ms; however, this difference failed to reach significance (n=7, $P = 0.54$, one-way ANOVA).

3.3 TTA-P2 inhibits rebound firing in TLE neurons

Rebound AP firing can be evoked in mEC layer II stellate neurons after injection of a short hyperpolarizing current step in increasing increments (Figure 2). APs evoked are thought to occur, at least in part, due to the de-inactivation of T-type Ca^{2+} channels during the hyperpolarizing step and subsequent activation of these channels upon membrane repolarization, driving neurons to firing thresholds[14]. Hyperpolarization induced an average of 1.3 ± 0.2 APs (n = 6) in control and 1.5 ± 0.2 APs (n = 8) in TLE. TTA-P2 (1 μM) application reduced rebound APs in control neurons to 0.7 ± 0.2 (n = 6; P<0.05). In contrast, in TLE neurons TTA-P2 (1 μM; n = 8) application resulted in the complete abolishment of evoked APs.

3.4 $Ca_V3.1$ channel isoform mRNA is increased in TLE

In order to determine if the changes in the efficacy of TTA-P2 in modulating neuronal excitability were due to increases in T-type Ca^{2+} channel message or expression, qPCR for the $Ca_V3.1$, 3.2, and 3.3 isoforms was performed on excised mEC layer II tissue from control and TLE brains. When compared to β-tubulin III controls, an almost 3- fold increase in $Ca_V3.1$ message was found in mEC layer II in TLE tissue as compared to controls (n = 3; $P < 0.0001$ one-way ANOVA; Figure 3A). In contrast to $Ca_V3.1$, no significant changes were seen for the $Ca_V3.2$ or $Ca_V3.3$ isoforms in TLE as compared to control tissue. This increase in T-type Ca^{2+} channel mRNA could likely correlate with an increase in $Ca_V3.1$ protein at the membrane and therefore, may account for the greater suppression of neuronal hyper-excitability recorded in TLE neurons upon TTA-P2 application as compared to controls.

3.5 Somatic T-Type Ca^{2+} channel properties are not different in TLE neurons.

To determine if T-type Ca^{2+} channel properties were altered within the somatic regions of TLE neurons T-type Ca^{2+} channel currents were recorded from brain slice preparations (Table 2). We found no change in T-type Ca^{2+} current amplitude between control and TLE mEC layer II stellate neurons (Figure 3B). Analysis of biophysical parameters also revealed no change in steady-state activation or inactivation parameters (Table 2). These findings suggest that alterations in T-type Ca^{2+} channel expression and activity are likely to occur at sites other than the soma, most likely along the dendrites as previously reported (Yaari et al., 2007). It is important to note that ionic currents recorded from brain slice preparations are likely compromised due to space clamp issues arising from the extensive neuronal processes. As such, the absence of any changes in the biophysical parameters of somatic T-type Ca^{2+} channel currents should be viewed with caution.

4.0 Discussion

In this study we investigated the role of T-type Ca^{2+} channels in facilitating neuronal hyperexcitability of medial entorhinal cortex (mEC) layer II stellate neurons. We confirmed previous observations that mEC layer II stellate neurons become hyperexcitable in TLE, firing more APs after depolarizing current injections and evoking bursts of APs after synaptic stimulation (Hargus et al., 2011). Our studies provide new information regarding the importance of T-type Ca^{2+} channels in facilitating this hyperexcitability. We show that 1) TTA-P2, a selective T-type Ca^{2+} channel antagonist (Kraus et al., 2010), reduces this neuronal hyperexcitability and suppresses burst firing in TLE neurons to a greater degree than that observed in control neurons, supporting a contributory role for T-type Ca^{2+} channels and 2) we show that $Ca_V3.1$ mRNA is upregulated by almost 3-fold, suggesting that $Ca_V3.1$ and not $Ca_V3.2$, the isoform associated with increases in hippocampal neuronal hyperexcitablity (A J Becker et al., 2008), is likely the candidate isoform responsible for facilitating increases in excitability within layer II stellate neurons of the mEC. These findings support a role for T-type Ca^{2+} channels in facilitating increased neuronal excitability in TLE and indicate regional specificity of isoform expression of T-type Ca^{2+} channels between the hippocampus and the EC.

T-type Ca^{2+} channels are known to contribute to the burst firing phenotype of many neuronal subtypes (Perez-Reyes, 2003). They are active around the resting membrane potential, where they can generate low threshold Ca^{2+} spikes (LTS) and the consequential triggering of sodium dependent APs (Cheong and Shin, 2013; Llinás, 1988). These studies have led to the generalization that T-type Ca^{2+} channels contribute predominately to the generation of LTS-mediated AP bursts, with little importance in establishing tonic firing modes, such as those attained during somatic current injection. Our studies show that T-type Ca^{2+} channels continue to be active during modes of tonic firing since inhibition of T-type Ca^{2+} channels with TTA-P2 caused significant reductions in tonic firing rates, in addition to suppression of synaptically evoked AP bursts. Recent studies support a role for T-type Ca^{2+} channels in facilitating tonic firing modes in thalamocortical and subiculum neurons (Deleuze et al., 2012; Joksimovic et al., 2017). T-type Ca^{2+} channel currents are thought to be the main contributors of Ca^{2+} current during the inter spike intervals, thereby contributing to firing frequencies (Swensen and Bean, 2003).

Many lines of evidence support a major role for T-type Ca^{2+} channels in the etiology of epilepsy. Many of these studies have focused on animal models of absence epilepsy (GAERS and WAG/Rij) where increased T-type Ca^{2+} channel expression and increases in T-currents have been reported and have been associated with the appearance of spike-wave discharges characteristic of absence seizures (Broicher et al., 2008; Talley et al., 2000; Tsakiridou et al., 1995). In the Coloboma SNAP25 deficient mouse model of absence epilepsy, the potentiation of T-type Ca^{2+} channel currents occurred before the onset of absence seizures, suggesting a causative role for T-type Ca^{2+} channels in the development of these specific seizures, and not a consequence of seizure activity (Zhang et al., 2004). Both the $Ca_V3.1$ and the $Ca_V3.2$ isoforms have been implicated in absence seizure generation (A J Becker et al., 2008; Ernst and Noebels, 2009; E. R. G. Sanabria et al., 2001; Su et al., 2002; Yaari et al., 2007). Over-expression of the $Ca_V3.1$ isoform in thalamic relay neurons resulted in an increase in T-current amplitude and increased the incidence of absence seizures in mice (Ernst et al., 2009).

In addition to extensive studies on the importance of T-type Ca^{2+} channels in absence epilepsy, T-type Ca^{2+} channels have also been implicated in TLE. In human patients with pharmaco-resistant epilepsy, robust T-type Ca^{2+} channel currents were recorded from isolated dentate gyrus neurons (Beck et al., 1998). In animal models of TLE, T-type Ca^{2+} channels have been reported to increase intrinsic bursting of CA1 pyramidal neurons following pilocarpine induced TLE (E. R. G. Sanabria et al., 2001; Su et al., 2002; Yaari et al., 2007). In these studies, T-channel density was increased 3-fold with no change in the density of any of the other types of neuronally expressed calcium channels. The emergence of spontaneous seizures in these TLE animals was associated with an increase and in $Ca_V3.2$ expression levels in CA1 pyramidal neurons. Furthermore, in mice lacking $Ca_V3.2$, the development of spontaneous seizures after SE were markedly attenuated (A J Becker et al., 2008), supporting a role for T-type Ca^{2+} channels in facilitating seizure generation. The findings of our study are consistent with these previous reports, supporting the notion that increases in T-type Ca^{2+} channel expression, or activity, contribute to hyperexcitability. Our study is the first that provides evidence for the contribution of T-type Ca^{2+} channel in controlling mEC layer II neuron activity, a subset of neurons that have received little

attention, but which serve as the primary input to the hippocampus circuitry. Since previous studies from our group have shown that rats that underwent status epilepticus, but did not develop spontaneous seizures were not different from control animals (Rajasekaran et al., 2007) our findings are not a consequence of status epilepticus, but instead a result of spontaneous seizures. Pro-excitatory alterations in mEC layer II excitability would ultimately provide an increase in excitatory signal into the hippocampus, allowing the mEC layer II neurons to play a crucial role in the initiation and propagation of seizure activity in TLE (Toyoda et al., 2013).

In contrast to studies within the hippocampus (A J Becker et al., 2008), our biochemical studies suggest that the main player contributing to the increases in neuronal excitability within the mEC is most likely to be $Ca_v3.1$. We detected a 3-fold increase in mRNA levels for $Ca_v3.1$ with no changes in $Ca_v3.2$ or $Ca_v3.3$ isoforms. Within subiculum neurons the prominent T-type Ca^{2+} channel isoform responsible for burst firing has been shown to be $Ca_v3.1$. Knock out of $Ca_v3.1$ lowered the fraction of bursting neurons when compared to WT controls (Joksimovic et al., 2017). Surprisingly, the increases in $Ca_v3.1$ mRNA were not reflected by increases in somatic T-channel recordings where no changes in current were recorded. Activation and inactivation parameters also remained unchanged. A likely reason for this discrepancy is the expression pattern of Ca_v channels, particularly $Ca_v3.1$, within a neuron. T-type Ca^{2+} channel expression has been widely documented in non-somatic neuronal regions, such as the dendrites where it is believed that T-type Ca^{2+} channels are expressed at high density and contribute to the amplification of excitatory inputs (Destexhe et al., 1996) We speculate that recording T-type Ca^{2+} channel currents at the dendrites would reveal increases in T-channel density as a result of increased mRNA. T-type Ca^{2+} channels are expressed at the axon initial segment (Bender et al., 2012; Bender and Trussell, 2009) and have been implicated in regulating presynaptic transmitter release in hippocampal and nociceptive circuitry (Huang et al., 2011; Jacus et al., 2012). Somatic T-type Ca^{2+} channel recordings would not have been able to assess the alterations in T-channel density as these distant sites.

Although mEC layer II neurons are spared after an epileptic insult they become hyperexcitable and contribute to the initiation and propagation of spontaneous ictal activity (Bertram and Cornett, 1993; Hargus et al., 2012). In TLE, a hyperexcitable mEC would lead to an increase in the magnitude of excitatory input into the DG (Kobayashi et al., 2003), resulting in an increase in hippocampal circuit excitation. Numerous mechanisms likely play a role in establishing and facilitating this hyperexcitability, including but not limited to: synaptic reorganization within the EC and hippocampus (Bear et al., 1996; Fountain et al., 1998), loss of local inhibitory interneuron populations (Du et al., 1995, 1993), and altered sodium channel function and expression (Hargus et al., 2013, 2011), however, the present study provides additional support for a role for T-type Ca^{2+} channel in contributing to the increases in neuronal hyperexcitability. Several lines of evidence have supported a role for T-type Ca^{2+} channel in controlling neuronal excitability within the hippocampus and subiculum (Joksimovic et al., 2017; E. R. Sanabria et al., 2001; Su et al., 2002; Yaari et al., 2007). Furthermore, inhibition of T-type Ca^{2+} channels can prevent tonic-clonic seizures in the maximal electroshock seizure model (Sakkaki et al., 2016) and delayed progression of seizures in an amygdala kindled model of TLE (Casillas-Espinosa et al., 2015). Together,

these studies provide rational to re-evaluate the use of highly potent and selective T-type Ca^{2+} channel antagonists for the treatment of seizures associated with TLE and not dismissed as solely a treatment for absence seizures.

Acknowledgments

Funding: This work was supported by the National Institutes of Health Grant NINDS RO1 NS103090 (MKP) and NS097726 to (EPR).

Abbreviation list:

TLE	temporal lobe epilepsy
mEC	medial entorhinal cortex
AP	action potential
LTS	low threshold spikes

References

Avoli M, D'Antuono M, Louvel J, KÖhling R, Biagini G, Pumain R, D'Arcangelo G, Tancredi V, 2002 Network and pharmacological mechanisms leading to epileptiform synchronization in the limbic system in vitro. Prog. Neurobiol 68, 167–207. [PubMed: 12450487]

Bear J, Fountain NB, Lothman EW, 1996 Responses of the superficial entorhinal cortex in vitro in slices from naive and chronically epileptic rats. J. Neurophysiol 76, 2928–2940. [PubMed: 8930245]

Beck H, Steffens R, Eiger CE, Heinemann U, 1998 Voltage-dependent Ca2+ currents in epilepsy. Epilepsy Res. 32, 321–32. [PubMed: 9761331]

Becker AJ, Pitsch J, Sochivko D, Opitz T, Staniek M, Chen C-C, Campbell KP, Schoch S, Yaari Y, Beck H, 2008 Transcriptional upregulation of Cav3.2 mediates epileptogenesis in the pilocarpine model of epilepsy. J. Neurosci 28, 13341–53. [PubMed: 19052226]

Becker AJ, Pitsch J, Sochivko D, Opitz T, Staniek M, Chen CC, Campbell KP, Schoch S, Yaari Y, Beck H, 2008 Transcriptional upregulation of Cav3.2 mediates epileptogenesis in the pilocarpine model of epilepsy. J. Neurosci 28, 13341–13353. [PubMed: 19052226]

Bender KJ, Trussell LO, 2009 Axon initial segment Ca2+ channels influence action potential generation and timing. Neuron 61,259–271. [PubMed: 19186168]

Bender KJ, Uebele VN, Renger JJ, Trussell LO, 2012 Control of firing patterns through modulation of axon initial segment T-type calcium channels. J.Physiol 590, 109–18. [PubMed: 22063631]

Bertram EH, Cornett J, 1993 The ontogeny of seizures in a rat model of limbic epilepsy: evidence for a kindling process in the development of chronic spontaneous seizures. Brain Res. 625, 295–300. [PubMed: 8275310]

Broicher T, Kanyshkova T, Meuth P, Pape H-C, Budde T, 2008 Correlation of T-channel coding gene expression, IT, and the low threshold Ca2+ spike in the thalamus of a rat model of absence epilepsy. Mol. Cell. Neurosci 39, 384–99. [PubMed: 18708145]

Casillas-Espinosa PM, Hicks A, Jeffreys A, Snutch TP, O'Brien TJ, Powell KL, 2015 Z944, a Novel Selective T-Type Calcium Channel Antagonist Delays the Progression of Seizures in the Amygdala Kindling Model. PLoS One 10, e0130012 10.1371/journal.pone.0130012 [PubMed: 26274319]

Cheong E, Shin H-S, 2013 T-type Ca2+ channels in normal and abnormal brain functions. Physiol. Rev 93, 961–92. [PubMed: 23899559]

Curia G, Lucchi C, Vinet J, Gualtieri F, Marinelli C, Torsello A, Costantino L, Biagini G, 2014 Pathophysiogenesis of mesial temporal lobe epilepsy: is prevention of damage antiepileptogenic? Curr. Med. Chem 21, 663–88. [PubMed: 24251566]

Deleuze C, David F, Béhuret S, Sadoc G, Shin H-S, Uebele VN, Renger JJ, Lambert RC, Leresche N, Bal T, 2012 T-type calcium channels consolidate tonic action potential output of thalamic neurons to neocortex. J. Neurosci 32, 12228–36. [PubMed: 22933804]

Destexhe A, Contreras D, Steriade M, Sejnowski TJ, Huguenard JR, 1996 In vivo, in vitro, and computational analysis of dendritic calcium currents in thalamic reticular neurons. J. Neurosci 16, 169–85. [PubMed: 8613783]

Dreyfus FM, Tscherter A, Errington AC, Renger JJ, Shin HS, Uebele VN, Crunelli V, Lambert RC, Leresche N, 2010 Selective T-type calcium channel block in thalamic neurons reveals channel redundancy and physiological impact of I(T)window. J. Neurosci. 30, 99–109. [PubMed: 20053892]

Du F, Eid T, Lothman EW, Kohler C, Schwarcz R, 1995 Preferential neuronal loss in layer III of the medial entorhinal cortex in rat models of temporal lobe epilepsy. J. Neurosci 15, 6301–6313. [PubMed: 7472396]

Du F, Whetsell WO Jr., Abou-Khalil B, Blumenkopf B, Lothman EW, Schwarcz R, 1993 Preferential neuronal loss in layer III of the entorhinal cortex in patients with temporal lobe epilepsy. Epilepsy Res. 16, 223–233. [PubMed: 8119273]

Ernst WL, Noebels JL, 2009 Expanded alternative splice isoform profiling of the mouse Cav3.1/alpha1G T-type calcium channel. BMC.Mol.Biol. 10, 53. [PubMed: 19480703]

Ernst WL, Zhang Y, Yoo JW, Ernst SJ, Noebels JL, 2009 Genetic enhancement of thalamocortical network activity by elevating alpha 1g-mediated low-voltage-activated calcium current induces pure absence epilepsy. J. Neurosci 29, 1615–1625. [PubMed: 19211869]

Fountain NB, Bear J, Bertram EH III, Lothman EW, 1998 Responses of deep entorhinal cortex are epileptiform in an electrogenic rat model of chronic temporal lobe epilepsy. J. Neurophysiol. 80, 230–240. [PubMed: 9658044]

Hargus NJ, Jennings C, Perez-Reyes E, Bertram EH, Patel MK, 2012 Enhanced actions of adenosine in medial entorhinal cortex layer II stellate neurons in temporal lobe epilepsy are mediated via A(1)-receptor activation. Epilepsia 53, 168–76. [PubMed: 22126400]

Hargus NJ, Merrick EC, Nigam A, Kalmar CL, Baheti AR, Bertram EH, Patel MK, 2011 Temporal lobe epilepsy induces intrinsic alterations in Na channel gating in layer II medial entorhinal cortex neurons. Neurobiol. Dis 41, 361–76. [PubMed: 20946956]

Hargus NJ, Nigam A, Bertram EH, Patel MK, 2013 Evidence for a role of Nav1.6 in facilitating increases in neuronal hyperexcitability during epileptogenesis. J. Neurophysiol 110, 1144–57. [PubMed: 23741036]

Huang Z, Lujan R, Kadurin I, Uebele VN, Renger JJ, Dolphin AC, Shah MM, 2011 Presynaptic HCN1 channels regulate Cav3.2 activity and neurotransmission at select cortical synapses. Nat. Neurosci 14, 478–86. [PubMed: 21358644]

Jacus MO, Uebele VN, Renger JJ, Todorovic SM, 2012 Presynaptic Cav3.2 channels regulate excitatory neurotransmission in nociceptive dorsal horn neurons. J. Neurosci 32, 9374–82. [PubMed: 22764245]

Joksimovic SM, Eggan P, Izumi Y, Joksimovic SL, Tesic V, Dietz RM, Orfila JE, DiGruccio MR, Herson PS, Jevtovic-Todorovic V, Zorumski CF, Todorovic SM, 2017 The role of T-type calcium channels in the subiculum: to burst or not to burst? J.Physiol 595, 6327–6348. [PubMed: 28744923]

Kim C-H, 2015 Cav3.1 T-type calcium channel modulates the epileptogenicity of hippocampal seizures in the kainic acid-induced temporal lobe epilepsy model. Brain Res. 1622, 204–216. [PubMed: 26111648]

Kobayashi M, Wen X, Buckmaster PS, 2003 Reduced inhibition and increased output of layer II neurons in the medial entorhinal cortex in a model of temporal lobe epilepsy. J. Neurosci 23, 8471–8479. [PubMed: 13679415]

Kraus RL, Li Y, Gregan Y, Gotter AL, Uebele VN, Fox SV, Doran SM, Barrow JC, Yang ZQ, Reger TS, Koblan KS, Renger JJ, 2010 In vitro characterization of T-type calcium channel antagonist

TTA-A2 and in vivo effects on arousal in mice. J.Pharmacol.Exp.Ther 335, 409–417. [PubMed: 20682849]

Llinás RR, 1988 The intrinsic electrophysiological properties of mammalian neurons insights into central nervous system function. Science 242, 1654–1664. [PubMed: 3059497]

Perez-Reyes E, 2003 Molecular physiology of low-voltage-activated t-type calcium channels. Physiol Rev 83, 117–161. [PubMed: 12506128]

Rajasekaran K, Kapur J, Bertram EH, 2007 Alterations in GABA(A) receptor mediated inhibition in adjacent dorsal midline thalamic nuclei in a rat model of chronic limbic epilepsy. J. Neurophysiol 98, 2501–8. [PubMed: 17855591]

Rutecki PA, Grossman RG, Armstrong D, Irish-Loewen S, 1989 Electrophysiological connections between the hippocampus and entorhinal cortex in patients with complex partial seizures. J.Neurosurg 70, 667–675. [PubMed: 2709106]

Sakkaki S, Gangarossa G, Lerat B, Françon D, Forichon L, Chemin J, Valjent E, Lerner-Natoli M, Lory P, 2016 Blockade of T-type calcium channels prevents tonic-clonic seizures in a maximal electroshock seizure model. Neuropharmacology 101,320–9. [PubMed: 26456350]

Sanabria ER, Su H, Yaari Y, 2001 Initiation of network bursts by Ca2+-dependent intrinsic bursting in the rat pilocarpine model of temporal lobe epilepsy. J.Physiol 532, 205–216. [PubMed: 11283235]

Sanabria ERG, Su H, Yaari Y, 2001 Initiation of network bursts by Ca 2 + -dependent intrinsic bursting in the rat pilocarpine model of temporal lobe epilepsy 205–216.

Segal M, Landis SC, 1974 Afferents to the septal area of the rat studied with the method of retrograde axonal transport of horseradish peroxidase. Brain Res. 82, 263–268. [PubMed: 4140749]

Siegel AM, Wieser HG, Wichmann W, Yasargil GM, 1990 Relationships between MR-imaged total amount of tissue removed, resection scores of specific mediobasal limbic subcompartments and clinical outcome following selective amygdalohippocampectomy. Epilepsy Res. 6, 56–65. [PubMed: 2357956]

Spencer SS, Spencer DD, 1994 Entorhinal-hippocampal interactions in medial temporal lobe epilepsy. Epilepsia 35, 721–727. [PubMed: 8082614]

Su H, Sochivko D, Becker A, Chen J, Jiang Y, Yaari Y, Beck H, 2002 Upregulation of a T-type Ca2+ channel causes a long-lasting modification of neuronal firing mode after status epilepticus. J. Neurosci 22, 3645–3655. [PubMed: 11978840]

Swensen AM, Bean BP, 2003 Ionic mechanisms of burst firing in dissociated Purkinje neurons. J. Neurosci 23, 9650–9663. [PubMed: 14573545]

Talley EM, Cribbs LL, Lee JH, Daud A, Perez-Reyes E, Bayliss DA, 1999 Differential distribution of three members of a gene family encoding low voltage-activated (T-type) calcium channels. J. Neurosci. 19, 1895–1911. [PubMed: 10066243]

Talley EM, Solorzano G, Depaulis A, Perez-Reyes E, Bayliss DA, 2000 Low-voltage-activated calcium channel subunit expression in a genetic model of absence epilepsy in the rat. Brain Res.Mol.Brain Res. 75, 159–165. [PubMed: 10648900]

Toyoda I, Bower MR, Leyva F, Buckmaster PS, 2013 Early activation of ventral hippocampus and subiculum during spontaneous seizures in a rat model of temporal lobe epilepsy. J. Neurosci 33, 11100–15. [PubMed: 23825415]

Tsakiridou E, Bertollini L, de Curtis M, Avanzini G, Pape HC, 1995 Selective increase in T-type calcium conductance of reticular thalamic neurons in a rat model of absence epilepsy. J. Neurosci 15, 3110–3117. [PubMed: 7722649]

Yaari Y, Yue C, Su H, 2007 Recruitment of apical dendritic T-type Ca2+ channels by backpropagating spikes underlies de novo intrinsic bursting in hippocampal epileptogenesis. J.Physiol 580, 435–450. [PubMed: 17272342]

Zhang Y, Vilaythong AP, Yoshor D, Noebels JL, 2004 Elevated thalamic low-voltage-activated currents precede the onset of absence epilepsy in the SNAP25-deficient mouse mutant coloboma. J. Neurosci 24, 5239–48. [PubMed: 15175394]

Highlights:

1. Medial entorhinal cortex (mEC) neurons within layer II are hyperexcitable in a rat model of temporal lobe epilepsy (TLE).
2. The selective T-type Ca^{2+} channel antagonist, TTA-P2, reduces this neuronal hyperexcitability and suppresses burst firing in TLE neurons to a greater degree than that observed in control neurons.
3. Cav3.1 mRNA is upregulated by almost 3-fold, suggesting that Cav3.1, and not Cav3.2 is likely the candidate isoform responsible for facilitating increases in excitability within layer II stellate neurons of the mEC.
4. Somatic T-channel currents are not altered suggesting increased expression in non-somatic neuronal regions.
5. Our findings support a contributory role for T-type Ca^{2+} channels in facilitating increased neuronal excitability in TLE. These studies provide rational to reevaluate the use of highly potent and selective T-type Ca^{2+} channel antagonists for the treatment of seizures associated with TLE.

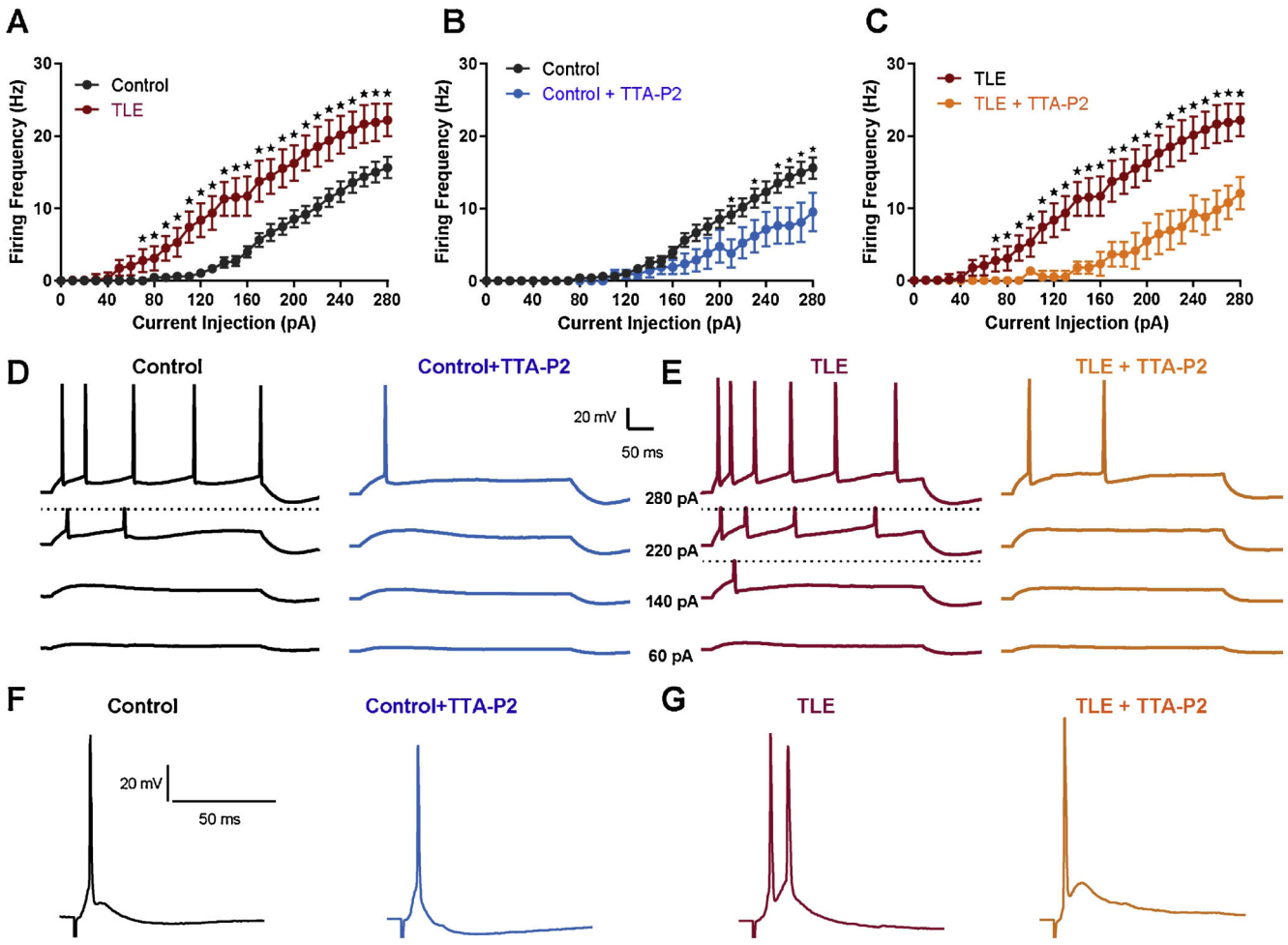

Figure 1. TTA-P2 ameliorates the hyper-excitability of mEC layer II stellate cells in TLE.

Action potentials were elicited using depolarizing current steps ranging from −20 to 280 pA. Firing frequency was increased and onset to firing was earlier in TLE (n = 13) compared to control (A; n = 16). Application of the selective T-type Ca^{2+} channel blocker, TTA-P2 (1 μM), reduced firing rates of control (n = 7) and TLE (n = 8) neurons to similar levels (B and C). Representative traces for control (D) and TLE (E) before and after application of TTA-P2, at current injection steps of 60, 140, 220, and 280pA. Action potentials were also evoked synaptically by stimulation of mEC layer III neurons. Representative traces for control (F) and TLE (G) before and after application of TTA-P2 (1 μM). Application of TTA-P2 reduced evoked action potentials in TLE neurons but had no effect on control neurons (right hand side F and G). Values represent means ± S.E.M. * P<0.05 (Students *t*-test or one-way ANOVA).

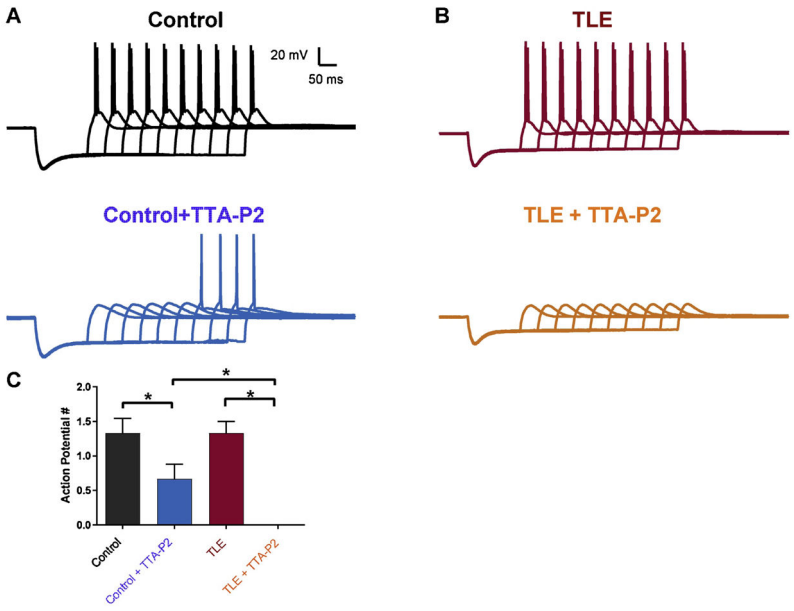

Figure 2. TTA-P2 strongly inhibits rebound action potentials in mEC layer II neurons.

Sustained hyperpolarizing pulses of increasing intensity were used to evoke rebound action potentials. Firing frequency for control (n = 6) and TLE (n = 8) neurons was not significantly different (A, B - top traces). Application of the selective T-type Ca^{2+} channel blocker, TTA-P2 (1 μM), reduced firing rates of control (n = 6) but completely abolished APs in TLE (n = 8) neurons. C. Bar chart showing effect of TTA-P2 (1 μM) on control and TLE neurons. Values represent means ± S.E.M. * $P<0.05$ (Students *t*-test).

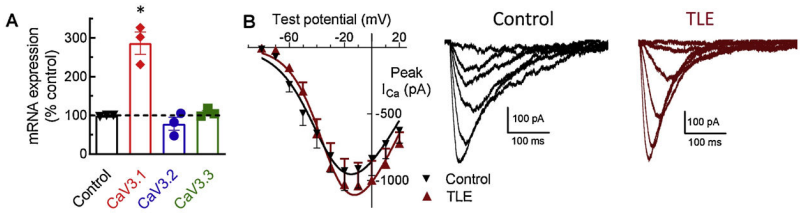

Figure 3. Cav3.1 mRNA is increased in TLE but somatic current density is unchanged.

(A) Cav3.1 mRNA expression is increased in TLE mEC layer II compared to control. (B) Somatic T-type Ca^{2+} channel current density recorded from mEC layer II neurons. Right panel shows example traces of T current family of currents. Values represent means ± S.E.M. * P<0.0001 (one-way ANOVA).

Table 1.

Effect of TTA-P2 on membrane properties of control and TLE neurons.

	RMP (mV)	IR(M Ω)	Threshold (mV)	Rheobase (pA)	Upstroke (V/s)	Amplitude (mV)	Width (ms)	n
Control	−60.3 ± 0.3	53.3 ±2.5	−44.1 ±0.8	144.4 ± 1.1	264.4 ± 5.3	41.1 ± 1.7	1.0 ± 0.0	16
Control+TTA-P2(1 μM)	−59.2 ± 0.5	51.2 ± 3.8	−40.9 ± 1.0 *	191.4 ± 2.6	264.4 ± 10.7	40.9 ± 2.2	1.0 ± 0.0	7
TLE	−62.1 ± 1.5	78.4 ± 10.7	−46.5 ± 2.0 #	85.0 ± 2.0 #	298.5 ± 9.1 #	43.0 ± 2.6	1.1 ± 0.1	13
TLE+TTA-P2 (1μM)	−60.1 ± 1.9	59.5 ± 10.3	−40.5 ± 2.1 *	207.5 ± 4.1 *	297.5 ± 16.1	45.9 ± 3.6	1.0 ± 0.0	8

# P<0.05 control v's TLE,

* P<0.05 Pre v's post TTA-P2 (Students *t*-test).

Table 2.

T-type Ca^{2+} channel current parameters in control and TLE mEC layer II neurons.

		Activation		Inactivation	
	Peak Amplitude (pA)	**V1/2 (mV)**	**k (mV)**	**V1/2 (mV)**	**k (mV)**
Control	−928 ± 147 (12)	−42.1 ± 3.2 (12)	−4.9 ± 0.3	−80.3 ± 1.6 (11)	7.6 ± 0.5
TLE	−1040 ± 174 (6)	−41.1 ± 8.7 (6)	−6.7 ± 0.7	−81.6 ± 2.0 (6)	7.5 ± 0.5